Impact of Transportation Electrification on the System's Dynamic Frequency Response

Preprint

Prasant Basnet,[1] Xin Fang,[1] and Nadia Panossian[2]

1 Mississippi State University
2 National Renewable Energy Laboratory

Presented at the 2023 IEEE Kansas Power and Energy Conference (KPEC)
Manhattan, Kansas
April 27-28, 2023

NREL is a national laboratory of the U.S. Department of Energy
Office of Energy Efficiency & Renewable Energy
Operated by the Alliance for Sustainable Energy, LLC

Conference Paper
NREL/CP-5400-85990
May 2023

This report is available at no cost from the National Renewable Energy Laboratory (NREL) at www.nrel.gov/publications.

Contract No. DE-AC36-08GO28308

Impact of Transportation Electrification on the System's Dynamic Frequency Response

Preprint

Prasant Basnet,[1] Xin Fang,[1] and Nadia Panossian[2]

1 Mississippi State University
2 National Renewable Energy Laboratory

Suggested Citation
Basnet, Prasant, Xin Fang, and Nadia Panossian. 2023. *Impact of Transportation Electrification on the System's Dynamic Frequency Response: Preprint*. Golden, CO: National Renewable Energy Laboratory. NREL/CP-5400-85990. https://www.nrel.gov/docs/fy23osti/85990.pdf.

NREL is a national laboratory of the U.S. Department of Energy
Office of Energy Efficiency & Renewable Energy
Operated by the Alliance for Sustainable Energy, LLC

This report is available at no cost from the National Renewable Energy Laboratory (NREL) at www.nrel.gov/publications.

Contract No. DE-AC36-08GO28308

Conference Paper
NREL/CP-5400-85990
May 2023

National Renewable Energy Laboratory
15013 Denver West Parkway
Golden, CO 80401
303-275-3000 • www.nrel.gov

NOTICE

This work was authored in part by the National Renewable Energy Laboratory, operated by Alliance for Sustainable Energy, LLC, for the U.S. Department of Energy (DOE) under Contract No. DE-AC36-08GO28308. Funding provided by the National Renewable Energy Laboratory. The views expressed herein do not necessarily represent the views of the DOE or the U.S. Government. The U.S. Government retains and the publisher, by accepting the article for publication, acknowledges that the U.S. Government retains a nonexclusive, paid-up, irrevocable, worldwide license to publish or reproduce the published form of this work, or allow others to do so, for U.S. Government purposes.

Cover Photos by Dennis Schroeder: (clockwise, left to right) NREL 51934, NREL 45897, NREL 42160, NREL 45891, NREL 48097, NREL 46526.

Impact of Transportation Electrification on the System's Dynamic Frequency Response

Prasant Basnet, Xin Fang
ECE Department
Mississippi State University
Starkville, MS, USA
{pb1052,xfang}@msstate.edu

Nadia Panossian
Center for Integrated Mobility Sciences
National Renewable Energy Laboratory
Golden, CO, USA
Nadia.Panossian@nrel.gov

***Abstract*—Transportation electrification is an integral component of the energy decarbonization transition. This paper investigates the impact of distributed energy resources (DERs), including distributed photovoltaics (DPV) and electric vehicles (EVs), in the primary frequency response of the power grid. Increasing DER adoption poses challenges to maintaining grid frequency stability. However, DERs' ability to provide fast frequency regulation services–primary frequency response (PFR) and secondary frequency response (SFR)–can be exploited to recover the frequency after an N-1 contingency event in the system. This paper also investigates the importance of a droop control strategy through dynamic models of DPV and EV to provide the primary frequency regulation services following the contingency event. A dynamic EV model, based on the PVD1 model Western Electricity Coordinating Council (WECC) introduced, has been used for the simulation. Further, DERs' primary frequency response is studied for five different cases of DER penetration levels after the system is exposed to the generator trip. Additionally, different frequency regulation capacities of EVs are analyzed. The studies show that an increment in DERs capacity providing effective PFR can improve the system frequency nadir and stabilize the frequency faster after the generation trip contingency.**

***Index Terms*—Distributed energy resources, distributed photovoltaic, electric vehicle, primary frequency regulation**

I. Introduction

Many countries have declared their carbon neutrality goals. The power sector has a defining role in reaching the zero-carbon emission target. The adoption of Distributed Energy Resources (DERs) in the form of distributed photovoltaics (DPV), energy storage, and electric vehicles has been increasing, as it plays a significant role in de-carbonizing the power sector [1]. However, the increased variable generation can replace the conventional fossil-fuel-based generation, lowering the overall system inertia. As a result, the requirement of the primary frequency regulation reserves augments following the sudden generation loss to stabilize the frequency and improve the frequency nadir [2]. Therefore, if DERs do not provide frequency regulation responses, the increased penetration level of DERs increases the burden of frequency regulation on conventional synchronous generators, which might be inadequate to provide this service in the future system. However, DERs can provide frequency regulation services to improve frequency stability. Moreover, the frequency regulation services from inverter-based DERs can be activated faster than mechanical governor-based frequency regulation [3]. There are frequency regulation services–primary frequency response (PFR) and secondary frequency response (SFR)–in real-time operation to balance the load and generation during contingency to recover the grid frequency [4]. A sudden loss of a generator or connection of a large load to the system causes an imbalance between demand and generation and subsequent deviation from the nominal frequency. The frequency deviation is first arrested by the inertial response of the overall system via PFR. Now, the error between the nominal resulting steady-state frequency and nominal frequency is corrected by SFR [5].

Especially, EVs are capable of providing up-regulation (discharging) and down-regulation (charging) to balance the demand and supply provided that they have the flexibility to attend grid services without compromising mobility demand [6]. Similarly, DPV can be a reliable and economically viable SFR provider under the high penetration of renewable energy [7]. Recent advancements in grid-supportive innovative inverter technology coupled with the modern plant control strategy have allowed DERs to provide voltage support and frequency response during various operation modes [8]. According to IEEE 1547-2018 Clause 6.5.2.7, DERs are required to have the technical capability to provide frequency-droop response similar to conventional generators [9]. Equipped with the battery energy storage system, EVs have the flexibility to provide fast frequency response to improve frequency stability. When vehicle-to-grid (V2G) service includes primary frequency control along with grid support, the system's overall stability remains invariable under critical contingencies [10]. EVs can also provide V2G frequency regulation services during peak load times if they are plugged in and have flexibility, as may be the case during long dwell times such as at workplace charging on commercial feeders or evening charging on residential feeders. There could be reservations about whether the V2G frequency regulation negatively impacts the battery life, charging times, or electric range. Battery degradation has been determined not accelerate significantly, as the capacity loss of battery will be about 35.03% for frequency regulation while it will be about 31.41% for EV driving and calendar aging if Level 1 charger is used at home [11]. However, user reservations about participation given impacts on charging times and electric range when providing services are still being explored. However, this V2G frequency regulation may negatively impact distribution network voltage profiles [12]. Moreover, increasing EV charging load during peak grid load times causes dips in the nodal voltage on the distribution system [13]. With very high adoption rates of EVs, the peak can even be shifted by EV charging and cause voltage drops during previously non-peak hours. [14]. Nevertheless, with smart charging management and grid-support capability of EV chargers, EV charging infrastructure can provide grid voltage stability and improve the distribution system along with other DERs [15].

DERs play an important role in the system's dynamic frequency response, improving nadir frequency and steady-state frequency [16]. PFR provided by these sources is pivotal for real-time power imbalance management as it uses a droop control strategy which is activated until the frequency deviations are more significant than the PFR dead band [17]. Both EV and DPV can provide primary regulation with this control strategy.

This paper studies the impact of DPV and EVs on primary frequency regulation services. Moreover, it focuses on the sensitivity of PFR concerning the percentage penetration levels of DPV and participating EVs for this study in the existing grid and the regulation capacities of EVs. The major contributions of this paper are summarized below:

- The impact of DPV and EV on the primary frequency regulation is analyzed under different DER penetration levels.
- The impact of increasing EV PFR capacities following N-1 contingency is analyzed.

The rest of this paper is organized as follows: Section II presents the dynamic models of DPV and EV. Section III performs the case studies on the sensitivities of DER penetration levels and EV regulation capacities. Section IV concludes the paper.

II. DPV AND EV DYNAMIC MODELS

The overall dynamic model of DPV and EV is added to ANDES [18], a power system electro-mechanical dynamics tool. The power flow and dynamics data of IEEE-39 bus system [19] are parsed and fed into the ANDES system. The dynamic models of PVD1 and EV are discussed below.

A. PVD1 model

PVD1 is a generic model introduced by the Western Electricity Coordinating Council (WECC) to represent the dynamic response of DPV. The current injection model has reactive and active power control and protection functionality. The model in Fig. 1 considers both PFR and SFR [20].

1) PFR: PFR uses droop control, i.e., when the frequency deviation is larger than a PFR Deadband, the DPV change its active power output accordingly. An additional power output P_{drp} is added to the generation output [12]:

$$P_{drp} = \begin{cases} \frac{(60 - db_{UF}) - f}{60} D_{DN} \; if \; f < 60 \\ \frac{f - (60 + db_{OF})}{60} D_{DN} \; if \; f > 60 \end{cases} \quad (1)$$

where db_{UF} and db_{OF} are the under-frequency and over-frequency deadband, respectively; and Ddn is the per-unit power output change to 1-p.u. frequency change (frequency droop gain).

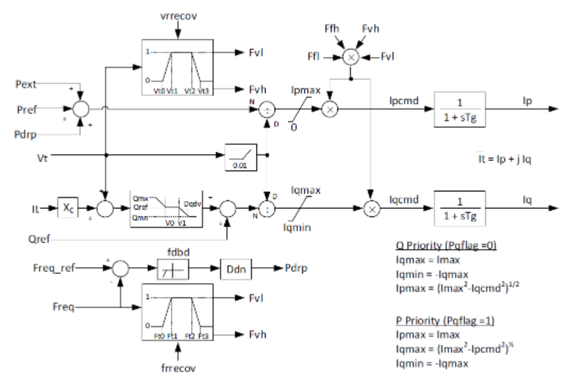

Fig. 1. Block diagram of PVD1 dynamic model

B. EV model

The EV model has been developed based on the Western Electricity Coordinating Council PVD1 model. This EV model can provide frequency regulation depending on the charging and discharging of EVs. In this model, the participation factor (pcap) determines the charging or discharging of EVs. The value of Pcap ranges from -1 to +1, where -1 represents EV's maximum power is 100% charging while +1 represents the 100% discharging. EVs can change the status of the charge to provide PFR. Furthermore, the state-of-charge (SOC) related block determines the current flowing in and out of the battery storage system [4]. This model provides PFR in the same way as described in subsection II-A1. The max power from charging an EV is linear between about 5% SOC and 85% SOC for level 2 charging. The EV model in this paper is an aggregation of many participating level 2 EV chargers for grid frequency response, so we assume that all vehicles are only charging and discharging between 5-85% SOC, so the maximum power can be linearly controlled. High power and DCFC are not considered here because it is assumed that users will not be wiling to participate and increase charge times when connected to fast chargers. It also assumes that there are sufficient participating charging stations such that vehicles are available according to the participation specified in each case.

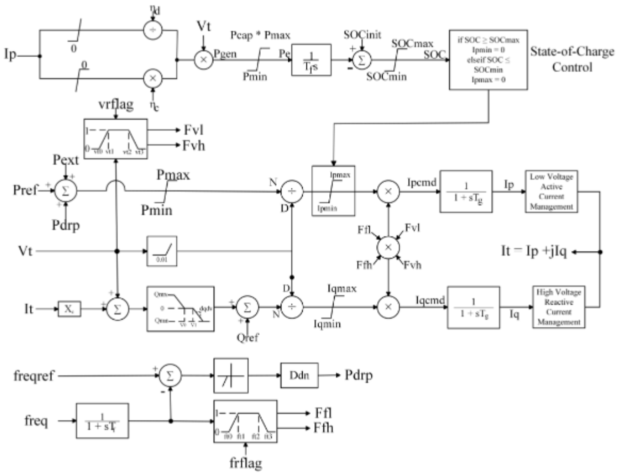

Fig. 2. Block Diagram of EV2 dynamic model including PFR

III. Case Studies

IEEE-39 bus system network has been used for the case study. This system has 10 synchronous generators and 46 lines.

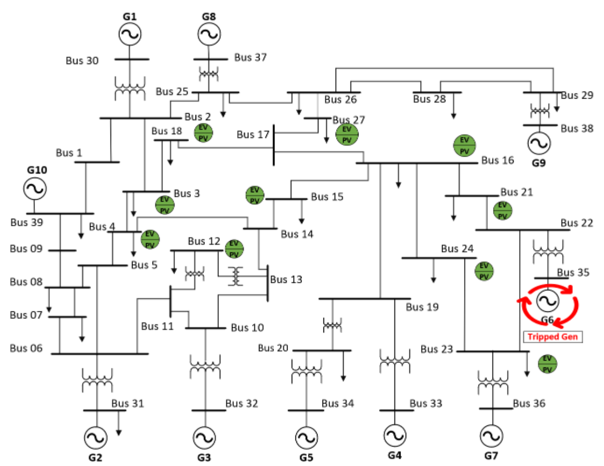

Fig. 3. Single Line Diagram of IEEE-39 bus transmission system

At first, five cases of different DER penetration levels were studied to observe the dynamic frequency response of the overall system when N-1 contingency occurs. 5% of active power regulation is provided by DPV and EV in each of these cases. At 5 seconds, Generator 6 with 687 MW power at bus 35 is tripped. The penetration level of 10%, 20%, 30%, 40%, and 50% is used to simulate the different DER penetration scenarios. The penetration level is calculated by equation 2.

$$\%penetration = \frac{\sum P_{DPV}}{\sum P_L} \tag{2}$$

where $\sum P_{DPV}$ is the total active power generated by distributed generation (DPV or EV) and $\sum P_L$ is the total active power consumed by loads.

Second, to observe the impact of the regulation capacity of EVs on PFR provision, the different participation levels of EVs in the system have been simulated at 10% DER penetration level in Case VI, and the frequency responses were noted. Fig. 4 shows the system's frequency response when the N-1 contingency is applied in the base case. It shows that the system's frequency dips to 59.827 Hz after Generator 6 is tripped at 5 seconds and the final frequency settles at 59.841 Hz.

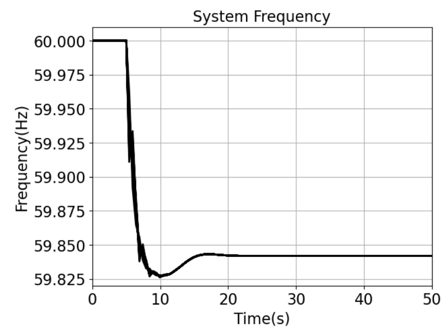

Fig. 4. Frequency Response of base case

A. Case I: 10 % penetration level

To introduce the 10% penetration level of DER in the system, 0.59 GW of DPV generation and 0.59 GW of EV load are added in the same buses (Bus 16, Bus 21). The dynamic frequency response after the N-1 contingency in Fig. 5 shows that the frequency nadir has reached 59.838 Hz and it settles at 59.85 Hz.

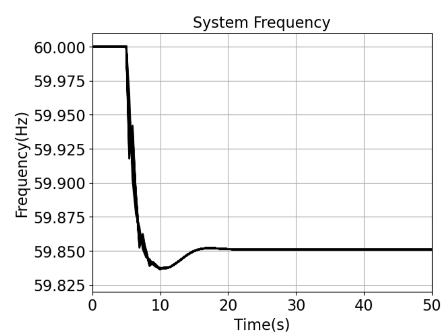

Fig. 5. Frequency Response with 10% penetration level

B. Case II: 20% Penetration Level

The DPV generation and EV capacity were increased to 1.17 GW by adding DPV and EV into more buses(Bus 15, Bus 16, Bus 21, Bus 23) to achieve a 20% penetration level. The frequency response after an N-1 contingency shows that the system's frequency nadir reaches 59.852 Hz and settles at 59.868 Hz.

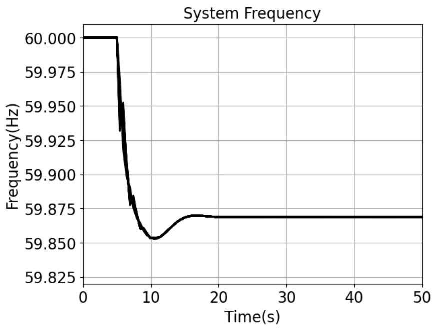

Fig. 6. Frequency Response with 20% penetration level

C. Case III: 30% Penetration Level

For 30% penetration, DPV and EV were added to buses 15, 16, 21, 23, 24, and 27. The total DPV and EV added to these buses amounts to 1.76 GW each. The dynamic frequency response shows the frequency nadir is 59.868 Hz and it settles at 59.897 Hz.

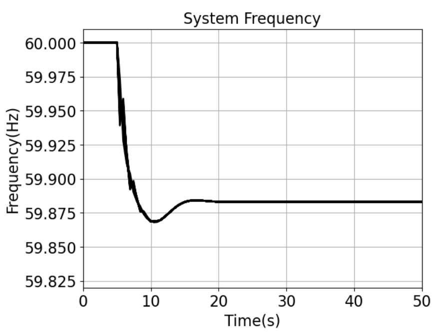

Fig. 7. Frequency Response with 30% penetration level

D. Case IV: 40% Penetration Level

The DPV generation and EV load were increased to 2.34 GW each to achieve a 40% penetration level. The frequency response after N-1 contingency shows the frequency nadir of the system reaches 59.882 Hz and settles at 59.897 Hz. DPV generation and EV load have been added to buses 3, 15, 16, 18, 21, 23, 24, and 27.

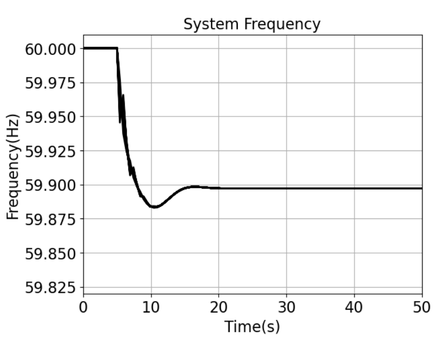

Fig. 8. Frequency Response with 40% penetration level

E. Case V: 50% Penetration Level

The DPV generation and EVs were increased to 2.93 GW each to achieve a 50% penetration level. The frequency response after N-1 contingency shows the frequency of the system reaches 59.898 Hz and settles at 59.912 Hz. PV generation and EVs' capacity have been added in buses 3, 4, 12, 15, 16, 18, 21, 23, 24, and 27. Table I shows the summary of simulation results under different cases.

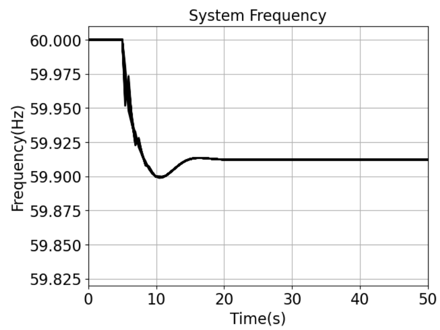

Fig. 9. Frequency Response with 50% penetration level

TABLE I
SUMMARY OF SIMULATION RESULTS

Case	DPV/EV(GW)	Penetration	f(Hz) nadir	Final f(Hz)
Base Case	0	0%	59.827	59.841
Case I	0.59	10%	59.838	59.85
Case II	1.17	20%	59.852	59.868
Case III	1.76	30%	59.868	59.883
Case IV	2.34	40%	59.882	59.897
Case V	2.93	50%	59.898	59.912

F. Case VI: EV Participation

In the preceding cases, the percentage of active power regulation was fixed at 5% for both EV and DPV. However, in this subsection, the regulation capacity of DPV is set to zero to test the performance of the EV regulation capability. The sensitivity of the participation of EVs has been tested to simulate system frequency response. As per Section II, the EVs' active power regulation can be controlled via charging or discharging. In this simulation, the regulation capacity is the whole EV fleet's capacity instead of the individual EV's capacity.

In this case, EV participation has been considered 5%, 10%, 20%, and 100% varying pcap values(i.e, -0.95,-0.9,-0.8,1). When pcap is -0.95, the power output of EVs can be changed to 95% charging, and the EVs can provide 5% of their rated active power as the regulation up services (from 100% charging to 95% charging). Similarly, the EVs participation is varied by 10% and 20% by changing the pcap values to -0.9 and -0.8. EVs can participate fully when the pcap value changes to 1. As a result, with the increasing participation, there will be an increase in headroom for EVs to decrease their charging. Fig. 9 shows the frequency response of the system at different participation levels of EV. When the participation increases, both the frequency nadir and stable frequency of the system after contingency improve. This can be justified by observing the EVs' active power output. Fig. 10 shows the active power output of EVs, which were added to the system.

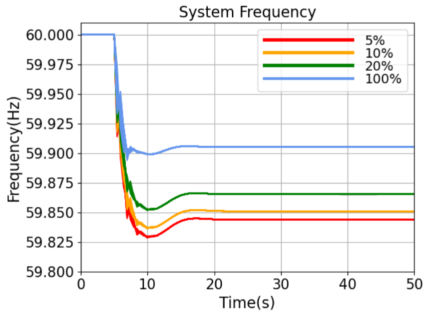

Fig. 10. Frequency Response with different EV Participation

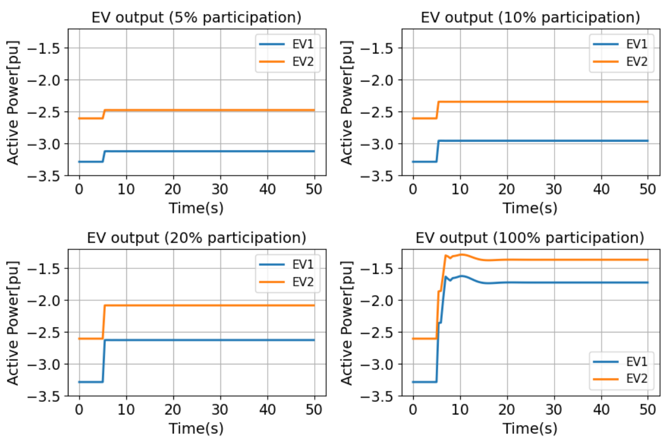

Fig. 11. Active Power Output of EVs at different participation

Fig 12 shows the output power from DPV without its participation in primary frequency regulation: the active power output remains the same even after an N-1 contingency event.

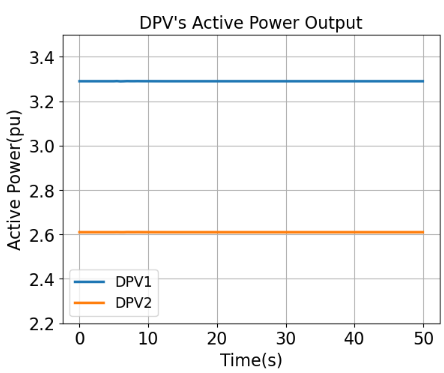

Fig. 12. Active Power Output of DPV without power regulation

IV. Conclusion

This paper discusses the impacts of EVs and DPV on the dynamic frequency response of the system. In this paper, the impact of increasing penetration of DERs on primary frequency response has been discussed. Simulation results show the increased penetration level improves the primary frequency response. As a result, the system frequency nadir and settling frequency improve, and the speed of frequency restoration following the contingency event becomes fast. Moreover, the increasing level of EV participation in the system improves the PFR. The flexibility of an EV charger to control the charging power of an EV can be utilized for frequency regulation services during contingency events. Several assumptions are taken for the study in this paper, but the results still show that EVs can provide PFR, and their participation also impacts PFR. Since EVs will be a mainstay of the future transportation system, their ancillary grid services, like frequency regulation, reactive power support, peak shaving, and load balancing, have to be studied in terms of techno-economic analysis and to determine which services are best suited to each type of vehicle and charging class. This study can be further extended to secondary frequency regulation provided by EVs under the different scenarios of penetration and participation. Furthermore, the impacts of providing grid services on EV battery lifetime will be studied with a longer-term integrated optimization and control simulation.

References

[1] "EPRI Advances Distributed Energy Resources with New Public Model." https://www.epri.com/about/media-resources/press-release/3QnkrHD4ptlzsKtF06U1Ta. [Online].

[2] J. H. Eto, J. Undrill, P. Mackin, R. Daschmans, B. Williams, B. Haney, R. Hunt, J. Ellis, H. Illian, C. Martinez, *et al.*, "Use of frequency response metrics to assess the planning and operating requirements for reliable integration of variable renewable generation," tech. rep., Lawrence Berkeley National Lab.(LBNL), Berkeley, CA (United States), 2010.

[3] A. Hoke and D. Maksimović, "Active power control of photovoltaic power systems," in *2013 1st IEEE Conference on Technologies for Sustainability (SusTech)*, pp. 70–77, IEEE, 2013.

[4] W. Wang, X. Fang, H. Cui, F. Li, Y. Liu, and T. J. Overbye, "Transmission-and-distribution dynamic co-simulation framework for distributed energy resource frequency response," *IEEE Transactions on Smart Grid*, vol. 13, no. 1, pp. 482–495, 2022.

[5] G. Zhang and J. McCalley, "Optimal power flow with primary and secondary frequency constraint," in *2014 North American Power Symposium (NAPS)*, pp. 1–6, IEEE, 2014.

[6] K. Kaur, M. Singh, and N. Kumar, "Multiobjective optimization for frequency support using electric vehicles: An aggregator-based hierarchical control mechanism," *IEEE Systems Journal*, vol. 13, no. 1, pp. 771–782, 2017.

[7] X. Fang, H. Yuan, and J. Tan, "Secondary frequency regulation from variable generation through uncertainty decomposition: An economic and reliability perspective," *IEEE Transactions on Sustainable Energy*, vol. 12, no. 4, pp. 2019–2030, 2021.

[8] C. Loutan, P. Klauer, S. Chowdhury, S. Hall, M. Morjaria, V. Chadliev, N. Milam, C. Milan, and V. Gevorgian, "Demonstration of essential reliability services by a 300-mw solar photovoltaic power plant," tech. rep., National Renewable Energy Lab.(NREL), Golden, CO (United States), 2017.

[9] IEEE, "IEEE standard for interconnection and interoperability of distributed energy resources with associated electric power systems interfaces," *IEEE-1547*, April 2018.

[10] J. C. Hernández, F. Sanchez-Sutil, P. Vidal, and C. Rus-Casas, "Primary frequency control and dynamic grid support for vehicle-to-grid in transmission systems," *International Journal of Electrical Power & Energy Systems*, vol. 100, pp. 152–166, 2018.

[11] D. Wang, J. Coignard, T. Zeng, C. Zhang, and S. Saxena, “Quantifying electric vehicle battery degradation from driving vs. vehicle-to-grid services,” *Journal of Power Sources*, vol. 332, pp. 193–203, 2016.

[12] Y. Liu, T. J. Overbye, W. Wang, X. Fang, J. Wang, H. Cui, and F. Li, “Transmission-distribution dynamic co-simulation of electric vehicles providing grid frequency response,” in *2022 IEEE Power & Energy Society General Meeting (PESGM)*, pp. 1–5, IEEE, 2022.

[13] R. R. Shrestha, B. Paudyal, P. Basnet, D. Niraula, B. Mali, and H. D. Shakya, “Impact assessment of electric vehicle integration: A case study of kathmandu valley,” in *2022 IEEE Kansas Power and Energy Conference (KPEC)*, pp. 1–6, IEEE, 2022.

[14] N. V. Panossian, H. Laarabi, K. Moffat, H. Chang, B. Palmintier, A. Meintz, T. E. Lipman, and R. A. Waraich, “Architecture for co-simulation of transportation and distribution systems with electric vehicle charging at scale in the san francisco bay area,” *Energies*, vol. 16, no. 5, p. 2189, 2023.

[15] N. Panossian, M. Muratori, B. Palmintier, A. Meintz, T. Lipman, and K. Moffat, “Challenges and opportunities of integrating electric vehicles in electricity distribution systems,” *Current sustainable/renewable energy reports*, vol. 9, no. 2, pp. 27–40, 2022.

[16] S. S. Guggilam, C. Zhao, E. Dall’Anese, Y. C. Chen, and S. V. Dhople, “Primary frequency response with aggregated ders,” in *2017 American Control Conference (ACC)*, pp. 3386–3393, IEEE, 2017.

[17] N. Gao, D. Gao, and X. Fang, “Manage real-time power imbalance with renewable energy: Fast generation dispatch or adaptive frequency regulation?,” *Power Systems, IEEE Transactions on*, 12 2022.

[18] H. Cui, F. Li, and K. Tomsovic, “Hybrid symbolic-numeric framework for power system modeling and analysis,” *IEEE Transactions on Power Systems*, vol. 36, no. 2, pp. 1373–1384, 2020.

[19] “IEEE 39-Bus system.” https://icseg.iti.illinois.edu/ieee-39-bus-system/. [Online].

[20] “Generic Models (PV Plants).” https://www.esig.energy/wiki-main-page/generic-modelspv-plants/. [Online].